ACS Combinatorial Science

Research Article

pubs.acs.org/acscombsci

Microgradient-Heaters As Tools for High-Throughput Experimentation

Robert Meyer,*[,†] Sven Hamann,[†] Michael Ehmann,[†] Sigurd Thienhaus,[†] Stefanie Jaeger,[†] Tobias Thiede,[‡,§] Anjana Devi,[‡,§] Roland A. Fischer,[‡,§] and Alfred Ludwig*[,†,‡]

[†]Institute for Materials, [‡]Materials Research Department, and [§]Inorganic Chemistry II, Faculty of Chemistry and Biochemistry, Ruhr-Universität Bochum, 44801 Bochum, Germany

ABSTRACT: A microgradient-heater (MGH) was developed, and its feasibility as a tool for high-throughput materials science experimentation was tested. The MGH is derived from microhot plate (MHP) systems and allows combinatorial thermal processing on the micronano scale. The temperature gradient is adjustable by the substrate material. For an Au-coated MGH membrane a temperature drop from 605 to 100 °C was measured over a distance of 965 μm, resulting in an average temperature change of 0.52 K/μm. As a proof of principle, we demonstrate the feasibility of MGHs on the example of a chemical vapor deposition (CVD) process. The achieved results show discontinuous changes in surface morphology within a continuous TiO_2 film. Furthermore the MGH can be used to get insights into the energetic relations of film growth processes, giving it the potential for microcalorimetry measurements.

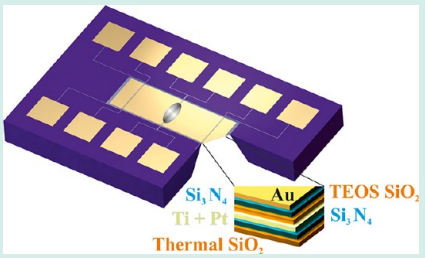

KEYWORDS: *TiO_2, high-throughput, microanalysis, microelectromechanical systems (MEMS), CVD*

1. INTRODUCTION

Combinatorial- and high-throughput experimentation methods are of importance for efficient materials research and demand for the development of new scientific instrumentation. In this respect the development of microelectro-mechanical systems (MEMS) tools for high-throughput experimentation, for example, Si cantilever arrays for stress measurements or hydrogen storage in thin films,[1,2] or microhot plates (MHPs) for thermal treatment of materials, is of interest.

MHPs, that is, membrane-type MEMS with integrated heaters and resistance sensors, are used for high-throughput thin film processing and in situ phase transformation characterization.[3] With similar devices microcalorimetry can be performed as well.[4] MHPs have been applied also in the area of high-throughput chemical vapor deposition (CVD) experiments to accelerate the identification of optimum processing parameters, like, for example, deposition temperature.[5] In the approach of Semancik et al.[6,7] a large number of MEMS devices were used simultaneously allowing for the systematic variation of the fabrication parameters. However, in this approach, for each intended processing temperature one MHP is needed. As a consequence of the design of suspended MHPs, a lateral temperature gradient occurs on the suspension-arms. During a CVD process this temperature gradient results in different microstructures and surface morphologies of the grown film. In this paper[7] the temperature gradient was a side-product of the inhomogeneous part of microheater devices. The temperature was deduced from the thin film morphology and was not measured directly.

"Large scale" in situ gradient annealing devices or temperature-gradient substrates were also reported, showing the advantage of these tools in combinatorial material science experiments.[8−10] Ohkubo et al.[10] reported about a setup having a temperature variation from 200 to 830 °C over 7.5 cm, giving a temperature gradient of 8.4 K/mm. Koida et al.[8] used a cantilever type substrate holder and a focused laser to achieve a temperature gradient of about 300 K, from 600 to 900 °C, over a distance of 11 mm. This corresponds to a temperature gradient of about 27 K/mm. When samples are processed on a gradient annealing device with a large temperature gradient, adequate high spatial resolution characterization technologies are necessary, to correlate the local processing temperature to the locally measured physical property: for example, if the measurement method has a spatial resolution of a micrometer or less, like, for example, scanning electron microscopy (SEM), scanning probe microscopy, nanoindentation, and so forth, a temperature gradient of 1000 K/mm could still be acceptable. In this case the temperature variation over one measurement point would be on the order of 1 K.

In this paper, the development of a microgradient-heater (MGH) for high-throughput experimentation and the results achieved by using this device in a CVD process are presented. The MGH chip is schematically shown in Figure 1a. It consists of a rectangular SiO_2/Si_3N_4 membrane (about 1 μm thick) which is supported by a rigid Si frame. The temperature gradient is induced by a central Pt thin film heater electrode. It is the aim to control this gradient in its lateral extension by the central heater electrode power and the membrane design, which will result in a specific temperature distribution. Two calibrated measurement electrodes quantify the temperature at

Received: May 2, 2012
Revised: August 9, 2012
Published: August 30, 2012

   dx.doi.org/10.1021/co3000488 | *ACS Comb. Sci.* 2012, 14, 531−536

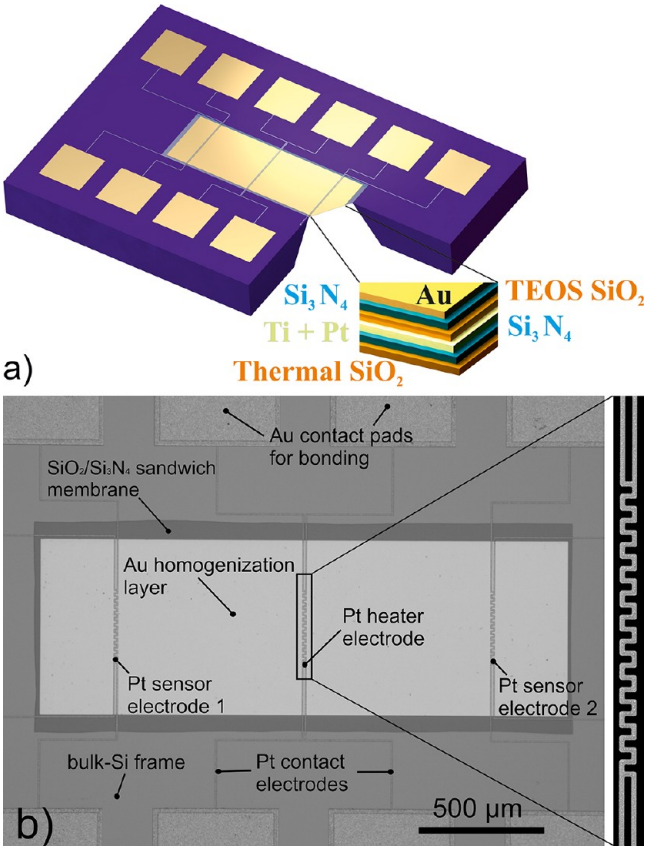

Figure 1. (a). Microgradient-heater chip design with membrane layer configuration. The lateral dimensions of the membrane are 2.2 mm × 0.85 mm. (b) Light-microscope image of a Au coated SiO_2/Si_3N_4 sandwich membrane (cf. Figure 2). The inset on the right shows a detailed SEM image of the Pt heater. The folded length of the meander is 294 μm, the folded width is 20 μm. To prevent for a heat drain from the membrane into the Si frame, the Au layer is deposited within the area of the free-standing membrane.

a given distance left and right from the central heater by measuring their temperature-dependent resistivity $R(T)$. Depending on the thermal conductivities of the materials which define the membrane, different temperature gradients can be designed. For the thermally insulating suspended SiO_2/Si_3N_4 sandwich membrane, a steep temperature gradient is expected correlated to the low thermal conduction coefficients of these materials. To achieve less steep temperature gradients, that is, a temperature profile which is extended over the complete membrane, additional layers, with higher thermal conductivity, for example, Au, were deposited on the SiO_2/Si_3N_4 membrane. Figure 1b shows a light microscope image of an Au-coated MGH; the inset on the right gives a detailed SEM image of the Pt heater structure.

The MGHs were calibrated by measuring the four-point resistance of their Pt heater- and sensor-electrodes as function of temperature prior to the experiment using a furnace equipped with a k-type thermocouple. The lateral temperature distribution of the membrane was measured using a thermo-camera. Thin TiO_2 films were grown on the calibrated MGHs, using metal−organic chemical vapor deposition (MOCVD). The resulting film morphologies were analyzed by SEM. Energy-dispersive X-ray investigation (EDX) was used to measure the element distribution after deposition.

2. EXPERIMENTAL PROCEDURES

2.1. Fabrication and Characterization of MGHs. MGHs were fabricated on four-inch ⟨100⟩ Si wafers (thickness 525 μm) by standard MEMS fabrication processes including photolithography, thin film deposition and etching, for details see Hamann et al..[3] A MGH chip (4.5 mm × 3 mm) consists of a stress-compensated, about 1 μm thick SiO_2/Si_3N_4 sandwich membrane (2.2 mm × 0.85 mm). The Si_3N_4 thin film has a tensile stress of about 1 GPa and the SiO_2 thin film has a compressive stress of about 300 MPa. We arranged the thickness ratio such that the stress of the sandwich membrane is near zero, with a low residual tensile stress to get a planar, free-standing membrane. Three Pt thin film meander electrodes (d = 100 nm) with a Ti adhesion layer (d = 10 nm) are embedded in the membrane (inset Figure 1a) and contacted by wire bonding on Au contact pads. The circuit paths of the three Pt electrodes each have a width of 6 μm (total 20 μm) and a folded length of 294 μm with a distance of 750 μm between each of the three Pt meanders. The temperature of the Pt heater electrode is controlled by measuring its resistivity in situ, using a personal computer with National Instruments LabView software and a digital multisource meter (Keithley model 2400). The Joule heating of the Pt meanders was performed by applying an electrical current. Calibration of the polynomial resistance-versus-temperature $R(T)$ relation of the Pt heaters and determination of the thermal coefficients was conducted in a furnace by external heating as reported in ref 3.

Because of the free-standing SiO_2/Si_3N_4 membrane, heat losses from the heated zone to the bulk Si frame are minimized. The low thermal mass of the heater allows heating/cooling rates up to 10^4 K/s. A maximum temperature of about 800 °C for short periods (up to 30 min) was determined for the MGHs. For temperatures up to 600 °C which are common for metal−organic chemical vapor deposition (MOCVD) processes,[11] the device is stable without degeneration of the membrane and the Pt heater, at least for several hours of operation (min. 28 h at 500 °C).

For the thermal analysis of the MGHs an infrared thermo-camera (InfraTec Variotherm) was used as well as the Pt temperature sensor electrodes (outer Pt electrodes). Because of the small size of MGHs, a 10 μm precision microscope-objective was required to gain the necessary magnification. In conjunction with the microscope-objective, the calibration of the thermo-camera (provided by manufacturer) is valid only up to 400 °C. In the following thermo-camera images, temperatures <400 °C are color-coded with respect to the measured temperatures, whereas temperatures >400 °C are plotted in pink. Because of the material-dependent thermal emission coefficient, the temperature information given by the thermo-camera is only valid for the Au-coated membrane, but neither for the Pt heater nor the Si frame.

The surface morphology of the grown films was investigated by SEM (Carl Zeiss LEO Supra 55 FEG) using an in-lens detector and a JEOL 5800 SEM using a secondary electron detector. EDX measurements were performed by an Inca X-act detector (Oxford instruments), attached to the JEOL SEM. The Au layers for temperature homogenization experiments were magnetron-sputtered (CMS 600/400 LIN, DCA) using photolithographically structured lift-off resist.

For the CVD experiments, a custom-made, horizontal, low-pressure, cold-wall reactor was used. A detailed description of the employed system was reported earlier.[12] To enable the use

dx.doi.org/10.1021/co3000488 | ACS Comb. Sci. 2012, 14, 531−536

of MGHs in this system, the inductively heated susceptor was replaced by an array of MGHs mounted on carrier chips. Bond pads on these carriers were connected by wire-bonding to provide electrical contact. The experimental parameters for the CVD deposition process were temperature and deposition time. All other parameters were kept constant. The metal organic complex $[Ti(OPri)_4]$ was used as single source precursor for the TiO_2 deposition.[13] The precursor was evaporated at a temperature of 40 °C and subsequently transported to the reaction zone using nitrogen (purity 6.0) as carrier gas with a flow rate of 50 sccm. The reactor pressure was set to 5 mbar.

3. RESULTS AND DISCUSSION

3.1. MGH Characterization. Because of the low heat conduction coefficient of the (SiO_2/Si_3N_4) membrane ($k_{SiO_2} \approx$ 1.4 W/m·K amorphous,[14] $k_{Si_3N_4} \approx$ 15 W/m·K[15]) the temperature gradient in the membrane perpendicular to the heater is steep (cf. Taylor et al. 790 K/70 μm = 11.3 K/μm[7]). The extension of the temperature gradient over the length of the membrane can be adjusted by additional layers, either on top or bottom of the sandwich membrane, which improves heat conduction. These layers need to be inert and thermally stable in the reactive environment at the temperature of deposition. Therefore noble metals or transition metal nitrides are a suitable choice as these materials are stable under common CVD conditions and exhibit reasonably high thermal conductivity to enhance the heat conduction. In the example shown, an Au (k_{Au} = 318 W/m·K bulk @ RT[11]) heat conduction layer was sputtered on top of the membrane, also serving as a substrate layer for the CVD-deposited film. The Au layer is sputtered on top of a Cr adhesion layer (10 nm) and has a total thickness of 400 nm. For the thermal decoupling of the membrane from the bulk Si frame it is necessary to leave a gap between the Au layer and the Si frame.

Figure 2 panels a and b show color-coded temperature profiles of two MGHs at temperatures of (a) T_{center} = 513 °C and (b) T_{center} = 605 °C as recorded by the thermo-camera. The experiments were conducted under ambient conditions. The temperature profile as a function of distance from the Pt heater was determined by thermal analysis using the IRBIS3 software and additionally controlled at two discrete points using the outer Pt electrodes as temperature sensors (red dots: (a) T_{left} = 179 °C, T_{right} = 181 °C; (b) T_{left} = 148 °C, T_{right} = 150 °C). The "shoulder" around the sensor in the left part of both thermo-camera pictures is due to contamination with dust particles during the measurement. The difference between the values determined by the thermo-camera and the Pt-temperature sensor on the right side is <5 K for both temperature set points. With increasing distance to the heater, the temperature decreases from (a) 513 to 100 °C over a distance of 845 μm and from (b) 605 to 100 °C over a distance of 965 μm. These results give an average temperature gradient of about (a) 0.49 K/μm and (b) 0.52 K/μm. The pink area extends about (a) ± 240 μm and (b) ± 350 μm to each side of the heater and indicates temperatures ≥400 °C, as described above. The borderline of this temperature region shows a biconvex shape. This shape is related to the proximity of the membrane edges to the bulk Si frame, where heat is partially conducted from the membrane into bulk Si. In the middle of the membrane the heat losses due to conduction have a minimum, leading to a flattened temperature gradient. The device exhibits a gradual

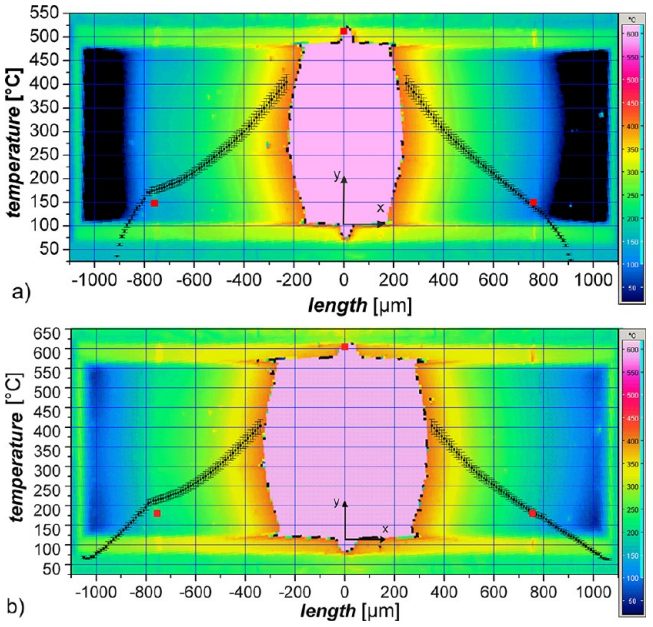

Figure 2. (a, b). Color-coded temperature distribution over an Au-coated MGH-membrane set to (a) T_{center} = 513 °C and (b) 605 °C, respectively, measured under ambient conditions. The temperature profile from the thermo-camera measurement is indicated by black dots with error bars. The red dots mark the temperatures measured with the Pt-electrodes on the membrane. The depicted MGHs are according to Figure 1b.

decline in temperature over the whole membrane. Heating the central heater electrode of an Au-coated MGH results in an almost symmetric temperature distribution, in *x*- and *y*-direction along the membrane. This is further confirmed by the two Pt temperature sensors (red dots in Figure 2). As expected from Fourier's law the width of the thermal gradient increases with increasing temperature.

Additionally we measured the temperature decline for a MGH in the CVD reactor at a flow of 40 sccm but without precursor at a pressure of 5 mbar. At a center temperature of T_{center} = 598 °C we obtained temperatures of T_{left} = 159 °C and T_{right} = 160 °C. This is surprising because we estimated the temperature gradient to be wider than under ambient conditions, because of much lower convection at reduced pressure. We assume two different reasons for this behavior:

(1) The temperatures measured under ambient atmosphere are increased because of the heat accumulation in the encapsulated volume below the membrane, because heated air below the device reduces thermal losses.

(2) Although the absolute pressure is only 5 thousandths of ambient conditions, the relatively high gas flow (40 sccm) in the quartz reactor leads to a constant heat drain by convection.

Considering this, the temperature profile during the CVD experiments is slightly lower than predicted by the fit function we applied for the Au coated MGH. We calculated a difference of 6 K at $T_{ambient}$ = 500 °C (T_{5mbar} = 494 °C) and 10 K at $T_{ambient}$ = 400 °C (T_{5mbar} = 390 °C). This deviation is considered during the following analysis of the CVD films.

The two equivalent temperature gradients of the device left and right to the central heater lead to the growth of directly comparable thin films, which then can be used for further processing or materials analysis.

Considering all the results determined by thermo-camera and Pt temperature sensors, the temperature distribution over a

dx.doi.org/10.1021/co3000488 | ACS Comb. Sci. 2012, 14, 531−536

MGH membrane is well-determined and suitable for further thin-film deposition experiments.

3.2. Deposition of TiO_2 Thin Films on MGHs by Chemical Vapor Deposition. TiO_2 films were deposited by thermal low pressure metal organic vapor deposition (LP-MOCVD) on MGHs. For CVD processes in general, film growth is strongly dependent on temperature and a variation of the deposition temperature has a huge impact on the structure and morphology of the deposited films. Therefore, the deposition temperature has to be carefully adjusted. Because of the defined thermal gradient along the MGH-membrane it is possible to fabricate thin films at a wide temperature range simultaneously, and the resulting properties can be studied as a function of deposition temperature. For example, the surface morphology varied for the TiO_2 films deposited on the MGH as a function of temperature. Figure 3 shows SEM micrographs

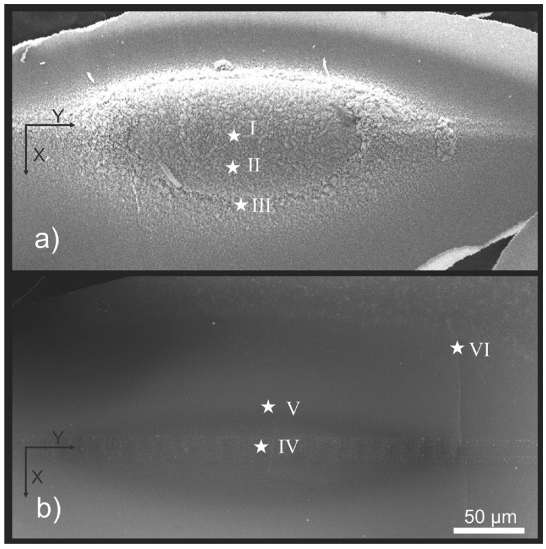

Figure 3. SEM top-view analysis of MGHs with TiO_2-coatings: (a) an Au-coated MGH processed at T_{center} = 600 °C and (b) an uncoated (i.e., no additional temperature homogenization layer) MGH processed at T_{center} = 500 °C. The heating meander is oriented in *y*-direction, the temperature gradient therefore forms in *x*-direction. Roman numbers indicate the locations of higher magnification SEM micrographs shown in Figures 4 and 5.

of two MGH membranes (membranes were extracted from the chip for characterization) after deposition of TiO_2 under different conditions. The MGH in (a) is an Au-coated membrane, processed at T_{center} = 600 °C for 5 min. The MGH in (b) is an uncoated membrane (i.e., no additional substrate layer), processed at T_{center} = 500 °C for 1 min. The roman numbers in Figure 3 mark the position of SEM micrographs of higher magnification, which are shown in Figure 4 and Figure 5, respectively. We used the fit function gained by the thermal characterization (Figure 2a,b), modified with the low pressure data to allocate discrete temperatures to the morphologies that are observed in the SEM images. The micrographs show morphology changes both in micro- (Figure 4) and in nanoscale (Figure 5). At 600 °C the TiO_2 film exhibits a cauliflower-like morphology showing round features at the surface (Figure 4 I). Around 525 °C (Figure 4 III) the TiO_2 displays a feather-edged-like surface morphology with sharp edges. At a temperature of about 565 °C (Figure 4 II) a discrete morphology change, from the rounded cauliflower- to

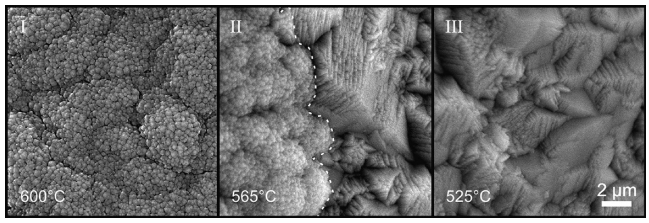

Figure 4. SEM top-view analysis of TiO_2 coating morphologies as a function of MGH temperature (p = 5 mbar, t = 5 min, T_{center} = 600 °C). Position of I, II, and III according to Figure 3a. The dashed line marks a morphology change at a grain boundary. Temperatures shown were calculated using the fit function derived from the thermal analysis.

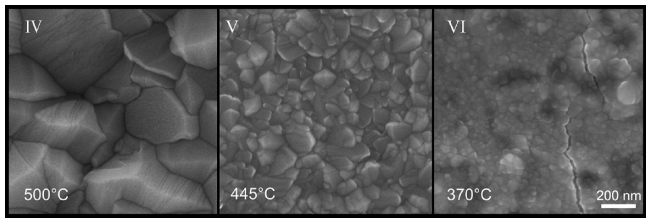

Figure 5. SEM top-view analysis of TiO_2 coatings showing the temperature-dependent grain size of TiO_2 deposited by CVD (p = 5 mbar, t = 1 min, T_{center} = 500 °C). Position of IV, V, and VI according to Figure 3b. Temperatures shown were calculated using the fit function derived from the thermal analysis.

the feather-edged-like surface, occurs at a grain boundary, without a notable difference in thickness. The grain boundary is highlighted by a dashed line. We correlate the regions of different morphology with a change in crystallinity and/or orientation of the TiO_2 films. Although this assumption could not be validated by X-ray diffraction (XRD), even when using a microcapillary with a spot size of around 800 μm (PANalytical XPert PRO), it is still reasonable, since it is well-known, that a change in deposition temperature has a drastic influence on film crystallinity.[16]

For TiO_2 films deposited at T_{center} = 500 °C no distinct change of the surface morphology in the microrange can be observed (Figure 5). At 500 °C the surface shows angular grains with sizes up to 600 nm (Figure 5 IV). The shape of the grains is constant for the whole deposited film, but the grain size is highly temperature-dependent, with decreasing size for decreasing deposition temperature. The nominal grain size decreases to around 150 nm for 445 °C (Figure 5 V) and 50 nm for 370 °C (Figure 5 VI). If the compound of membrane and deposited film exhibits high stress states, the stresses can be relaxed by cracking, either of the membrane or the deposited film, or both. The TiO_2 film deposited at 500 °C on SiO_2 shows this type of stress compensation, illustrated by the development of cracks in the TiO_2 film after cooling to room temperature (RT) (Figure 3b and Figure 5 VI). High stresses can also lead to membrane bending. This was further confirmed by light microscopy images (not shown).

To determine the size of the area on the MGH membrane where TiO_2 has been deposited, an EDX intensity distribution for Ti was measured for two samples. Figure 6 shows a comparison of a SEM image and the corresponding EDX intensity distribution of Ti for two MGHs without thermal homogenization layer (i.e., Si_3N_4 is the top layer of the membrane). Both MGHs were coated for 1 min, the one in Figure 6a,c at T_{center} = 600 °C and the one in Figure 6b,d at

dx.doi.org/10.1021/co3000488 | ACS Comb. Sci. 2012, 14, 531−536

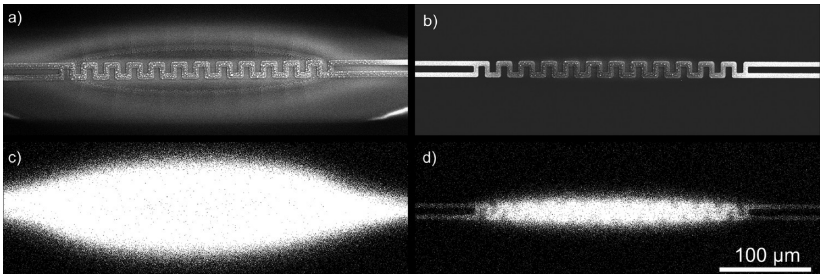

Figure 6. Low magnification SEM images of two uncoated (i.e., no additional temperature homogenization layer) MGHs after CVD TiO_2 deposition: (a) 600 °C, 1 min, (b) 400 °C, 1 min and corresponding EDX intensity distributions of Ti in (c) and (d). The meanders have a width of 6 μm and a folded length of 294 μm.

T_{center} = 400 °C. The bright pixels in the EDX intensity plots visualize detected Ti. Using this information the actual TiO_2 coated area can be determined. In Figure 6d the heater contour is visible because of the Ti adhesion layer of the Pt heater structure.

Figure 7 shows a SEM cross-section of the CVD film shown in Figure 6a,c. The TiO_2 thickness in the center is about 1.8 μm, from which an average deposition rate of 30 nm/s can be calculated. The film thickness is decreasing to below 100 nm over a distance (x-direction) of around 120 μm.

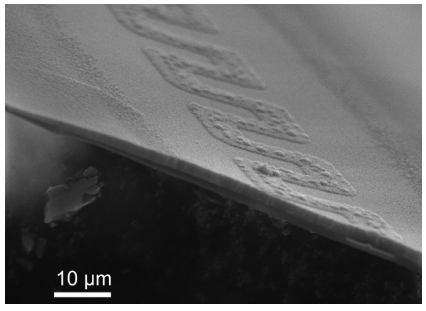

Figure 7. Cross-section SEM image of the MGH membrane without homogenization layer, shown in Figure 6a,c, processed at 600 °C for 1 min. The thickness in the center is about 1.8 μm.

3.2. Microcalorimetric Examination of a CVD Process.

The power applied to the middle Pt heater is controlled in real-time, and it was observed that the applied energy has to be continuously increased during the CVD process to maintain the desired temperature when film growth is occurring. At the beginning the heater was set to T_{center} = 500 °C. The set point was reached with a slow heating rate of ≈ 27 K/s after 18 s with an overshoot of around 10 K. The temperature was then held at set point for 35 s (oscillating at 509 ± 2 °C due to inertia of the controller). To introduce the precursor into the CVD process chamber, the carrier gas flow has to be rerouted, leading to a short pressure drop in the reactor. Because of the decrease of heat loss by conduction, the controller reregulates the input current, leading to an abrupt drop in heating power and thus in temperature. After introducing the precursor to the reactor-zone, an incubation period of about 15 s is needed for the nucleation process to begin (x = 0 s in Figure 8). After the incubation period, nucleation starts and the energy consumption increases, thus the applied electrical power is increased as can be seen in Figure 8.

To keep the deposition temperature constant, the electrical energy applied to the Pt heater had to be further increased during the deposition process. The reason for this is the very small thermal mass of the MGH, where even small energy losses can be directly observed. These losses are determined by a decrease of the heater temperature and thus its electrical resistance. Concerning this, the energy needed to set the heater to its target temperature can be regarded as a parameter describing the energy dissipation of the system due to film growth during the CVD process. Further the energy needed to decompose the precursor and initiate nucleation and grain growth can be correlated to the electrical energy that has to be added during film growth, which allows investigating the energy dissipation as function of deposition material and precursor. This use of the MGHs is related to the use of MHPs for similar nanocaloric measurements, for example, to determine structural transformations in thin films by determining dissipated energy from the heater into deposited films.[4]

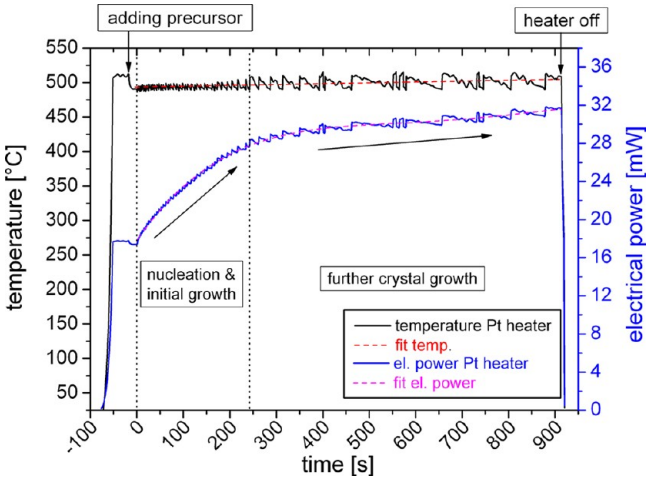

Figure 8. Heater temperature and electrical power supplied to the Pt heater as function of time are presented for a CVD process (deposition time 15 min). While the temperature stays almost constant, the time-dependent values for electrical power, to keep that temperature against the energy losses, describe a polynomial curve.

This statement is supported by Figure 8, where the Pt heater temperature (black) and the electrical power (blue) of a CVD experiment are presented. Functions (linear for temperature and polynomial for electrical power) were fitted to the data to clarify the general trend. While the temperature as a function of time is only slightly increasing from a start temperature of 494 °C (x = 0 s) to a final temperature of 504 °C, the electrical power applied to the heater increases over time from 17.4 mW to 31.7 mW, showing a polynomial increase. The temperature increases about 2% from the start to the end of the experiment, while the increase in heating power is 82.2%.

dx.doi.org/10.1021/co3000488 | ACS Comb. Sci. 2012, 14, 531−536

The steps within the curve for both parameters originate from the interaction between the software controller and the electrical power supply. When energy is transferred from the heater into film growth the heater temperature decreases. Since the electrical supply for the Pt heater has an additional controller inside, the electrical current is kept constant while the electrical voltage required to generate the current is slightly decreased. The step-like shape of the curves is therefore not a consequence of the CVD process.

The deposition process can be divided in two sections. The first section is characterized by a fast increase in electrical power. We correlate this steep slope section of the power curve mainly to diffusion, nucleation, and initial growth. When nucleation and initial film growth start, a large amount of energy is required to compensate for the energy dissipation. This relationship is qualitatively known from the literature, where nucleation consumes a much higher amount of energy than grain growth.[11]

After 240 s, the slope of the electrical power curve and thus the dissipated energy flattens to an almost linear behavior. This increase is attributed to the further crystal growth (i.e., the constantly increasing thermal mass).

This is only a qualitative review of the CVD processes, but it shows that if certain parameters like mass, density, nucleation energy, and so forth are known or calculated, the MGH can also be used to analyze the caloric and kinetic characteristics during a CVD process.

4. CONCLUSION AND OUTLOOK

The development and characterization of MGH and first results on TiO_2 thin film deposition by CVD were presented. In dependence of the MGH membrane temperature, different surface morphologies were identified. Furthermore, a distinct change in the micromorphology was found for a film deposited at 600 °C. These results prove that using a MGH as susceptor allows to rapidly screen within a defined temperature range to find the ideal deposition temperature for the particular application and thus is an interesting tool especially for high-throughput experimentation in terms of screening for temperature- or precursor-dependent properties. Finally the applicability of MGHs for the use as CVD process characterization tool was shown on the energetic analysis of a TiO_2 MOCVD.

By applying slight variations in design and/or materials used for the fabrication of the MGH, the device could be further tailored toward the need of the user, for example, steeper or smoother temperature gradient and adjusted MGH coating. A further improvement of the MGH would be the implementation of additional Pt heaters/electrodes to further manipulate and validate the temperature gradient along the membrane. A change of the heater design and/or material could allow to increase the achievable temperatures with MGH and to adjust the expansion of interesting temperature regions for different purposes.

AUTHOR INFORMATION

Corresponding Author

*E-mail: robert.meyer@rub.de (R.M.), alfred.ludwig@rub.de (A.L.).

Notes

The authors declare no competing financial interest.

ACKNOWLEDGMENTS

MEMS processes were partially performed by the caesar Micro Systems Technology Group, Bonn, Germany.

REFERENCES

(1) Ludwig, A.; Cao, J.; Brugger, J.; Takeuchi, I. MEMS tools for combinatorial materials processing and high-throughput characterization. *Meas. Sci. Technol.* **2005**, *16*, 111−118.

(2) Ludwig, A.; Cao, J.; Savan, A.; Ehmann, M. High-throughput characterization of hydrogen storage materials using films on micromachined Si substrates. *J. Alloys Compd.* **2007**, *446*−*447*, 516−521.

(3) Hamann, S.; Ehmann, M.; Thienhaus, S.; Savan, A.; Ludwig, A. Micro-hotplates for high-throughput thin film processing and in situ phase transformation characterization. *Sens. Actuators, A* **2008**, *147*, 576−582.

(4) McCluskey, P. J.; Vlassak, J. Combinatorial nanocalorimetry. *J. Mater. Res.* **2010**, *25*, 2086−2100.

(5) Lahr, D. L.; Hertz, J. L.; Semancik, S. A Combinatorial Study of Thin-Film Process Variables Using Microhotplates. *J. Microelectromech. Syst.* **2010**, *19*, 239−245.

(6) Semancik, S.; Cavicchi, R. E.; Kreider, K. G.; Suehle, J. S.; Chaparala, P. Selected-area deposition of multiple active films for conductometric microsensor arrays. *Sens. Actuators, B* **1996**, *34*, 209−212.

(7) Taylor, C. J.; Semancik, S. Use of Microhotplate Arrays as Microdeposition Substrates for Materials Exploration. *Chem. Mater.* **2002**, *14*, 1671−1677.

(8) Koida, T.; Komiyama, D.; Koinuma, H.; Ohtani, H.; Lippmaa, M.; Kawasaki, M. Temperature-gradient epitaxy under in situ growth mode diagnostics by scanning reflection high-energy electron diffraction. *Appl. Phys. Lett.* **2002**, *80*, 565−567.

(9) Thienhaus, S.; Hiergeist, R.; Savan, A.; Ludwig, A. Design and application of gradient annealing devices for the parallel thermal processing of Fe/Pt multilayers. *Mater. Res. Soc. Symp. Proc.* **2006**, *894*, 0894-LL01-04.1.

(10) Ohkubo, I.; Christen, H. M.; Kalinin, S. V.; Jellison, G. E., Jr.; Rouleau, C. M.; Lowndes, D. H. High-throughput growth temperature optimization of ferroelectric $Sr_xBa_{1-x}Nb_2O_6$ epitaxial thin films using a temperature gradient method. *Appl. Phys. Lett.* **2004**, *84*, 1350−1352.

(11) Pierson, H. O. *Handbook of Chemical Vapor Deposition (CVD): Principles, Technology, and Application*; Noyes Publications: Park Ridge, NJ, 1992.

(12) Devi, A.; Rogge, W.; Wohlfahrt, A.; Hipler, F.; Becker, H. W.; Fischer, R. A Study of Bisazido(dimethylaminopropyl)gallium as a Precursor for the OMVPE of Gallium Nitride Thin Films in a Cold-Wall Reactor System under Reduced Pressure. *Chem. Vap. Deposition* **2000**, *6*, 245−252.

(13) Babelon, P.; Dequiedt, A. S.; Mostéfa-Sba, H.; Bourgeois, S.; Sibillot, P.; Sacilotti, M. SEM and XPS studies of titanium dioxide thin films grown by MOCVD. *Thin Solid Films* **1998**, *322*, 63−67.

(14) Lee, S. M.; Cahill, D. G.; Allen, T. H. Thermal conductivity of sputtered oxide films. *Phys. Rev. B* **1995**, *52*, 253−257.

(15) Kunter, J.; Jachimowicz, A.; Kohl, F.; Jakoby, B. Determining the thin-film thermal conductivity of low temperature PECVD silicon nitride. *Eurosensors XX Conference* **2006**, 388−391.

(16) Chen, S.; Bianton, T. N.; Castro, T. Ultrahigh vacuum metalorganic chemical vapor deposition growth and in situ characterization of epitaxial TiO_2 films. *J. Vac. Sci. Technol. A* **1993**, *11* (5), 2419−2429.